Research Square

Preprints are preliminary reports that have not undergone peer review.
They should not be considered conclusive, used to inform clinical practice,
or referenced by the media as validated information.

Effects of Riociguat on Ovarian Ischemia–Reperfusion Injury: Modulation of Oxidative Stress, Inflammation, and Endocrine Function in a Rat Model

Meltem ALPAY

meltem.alpay@erdogan.edu.tr

Recep Tayyip Erdogan University

Esra DENİZ

Recep Tayyip Erdogan University

Mehtap ATAK

Recep Tayyip Erdogan University

Zehra TOPAL SUZAN

Recep Tayyip Erdogan University

Eda YILMAZ KUTLU

Recep Tayyip Erdogan University

Mazhar ÖZKAN

Research Article

Keywords:

Posted Date: July 22nd, 2026

DOI: https://doi.org/10.21203/rs.3.rs-10242754/v1

License: This work is licensed under a Creative Commons Attribution 4.0 International License.
Read Full License

Additional Declarations: No competing interests reported.

Abstract

Background:

Ovarian torsion is a gynecological emergency in which ischemia and reperfusion cause tissue damage through oxidative stress and microvascular dysfunction. Riociguat, a soluble guanylate cyclase (sGC) stimulator, enhances cyclic guanosine monophosphate (cGMP) production and may protect against ischemia-reperfusion (I/R) injury. This study evaluated the effects of riociguat on ovarian I/R injury in rats.

Methods:

Forty-seven Wistar albino rats were randomly assigned to six groups: Control, Sham, Ischemia, I/R, and I/R treated with riociguat at 3 mg/kg (IRR-3) or 10 mg/kg (IRR-10). Ovarian ischemia was induced by adnexal compression for 3 hours followed by 3 hours of reperfusion. Riociguat was administered orally at the 90th minute of ischemia. Oxidative stress, hormonal, inflammatory, histopathological, and immunohistochemical parameters were evaluated. Statistical significance was set at $p < 0.05$.

Results:

TBARS levels increased after ischemia and I/R ($p < 0.001$) and decreased following riociguat treatment ($p < 0.05$). GSH levels differed among groups ($p < 0.001$), with the highest levels in the IRR-10 group ($p < 0.05$). Serum LH levels were highest in the I/R group ($p < 0.001$) and decreased after riociguat treatment ($p < 0.05$). FSH levels were higher in the IRR-10 group than in the ischemia, I/R, and IRR-3 groups ($p < 0.05$). Estradiol levels decreased after ischemia and I/R ($p < 0.05$) but increased following IRR-10 treatment ($p < 0.05$). IL-10 levels increased in the IRR-10 group compared with the ischemia group ($p = 0.001$). Histopathological analysis showed increased vascular congestion ($p < 0.001$), edema, hemorrhage, and follicular degeneration ($p < 0.05$), whereas necrosis increased only in the IRR-3 group ($p = 0.049$). eNOS expression was lower in the IRR-10 group than in the ischemia group ($p = 0.0013$).

Conclusions:

Riociguat reduced oxidative stress ($p < 0.05$), enhanced antioxidant capacity ($p < 0.001$), improved endocrine function ($p < 0.05$), and promoted anti-inflammatory responses ($p = 0.001$), providing partial protection against ovarian I/R injury. Although these findings are consistent with sGC stimulation, direct activation of the NO–sGC–cGMP pathway was not demonstrated.

1. Introduction:

Ovarian torsion is a gynecological emergency that can affect women of all ages and accounts for approximately 2.7% of all such cases (1–4). It occurs as a result of the complete or partial rotation of the adnexa—the ovary and its supporting structures—leading to impaired blood flow and subsequent ischemic changes in the ovarian tissue (3). Ovarian torsion most frequently affects women of reproductive age. For the preservation of ovarian function and the prevention of severe morbidity, early diagnosis and prompt surgical intervention are essential (3).

Various factors may predispose individuals to ovarian torsion, including ovarian cysts, excessive ovarian stimulation, pregnancy, elongated oviducts, hypermobility of the adnexa due to mesosalpinx and mesovarium, hyperlaxity of the tuba-ovarian and infundibulopelvic ligaments, a history of adnexal torsion, and tubal ligation (5, 6).

The main goal of treatment for ovarian torsion, which is frequently seen in women of reproductive age, is to preserve ovarian function; the recommended course of action to achieve this goal is detorsion. Recent findings indicate that normal ovarian function can be restored after detorsion, even in the presence of blue-black discoloration. Therefore, excision is not recommended unless significant gelatinous necrosis is observed (1, 3, 7). Misdiagnosis or delay in treatment may result in peritonitis, ovarian loss (8), and even death (9). Therefore, ovarian torsion is an emergency that directly affects both the life and fertility of the person.

Ischemia in the ovary occurs during torsion, while reperfusion begins with detorsion. However, ischemia/reperfusion (I/R) injury may occur in the ovary following detorsion. The ischemic phase is characterized by hypoxia and cellular acidosis (10, 11), whereas the reperfusion phase involves neutrophil infiltration and the generation of reactive oxygen species (ROS) (10, 12, 13). During reperfusion, ROS interact with nitric oxide (NO)—a key mediator in numerous cellular processes and vascular smooth muscle relaxation—leading to the formation of highly reactive and potentially cytotoxic compounds such as peroxynitrite ($ONOO^-$) and nitrogen trioxide (N_2O_3)(14, 15).

The NO-soluble guanylate cyclase (sGC)-cyclic guanosine monophosphate (cGMP) pathway provides vasodilation in the vessels. NO stimulates sGC, which converts guanosine triphosphate (GTP) to cGMP, promoting the relaxation of vascular smooth muscle cells. However, I/R injury decreases NO levels and impairs its production, thereby disrupting the NO–sGC–cGMP pathway and contributing to endothelial dysfunction (14, 16).

sGC stimulators can potentiate the effects of endogenous NO by sensitizing sGC (17). One such agent, Riociguat (Adempas®), is approved for the treatment of inoperable or persistent chronic thromboembolic pulmonary hypertension and pulmonary arterial hypertension (18).

Given the central role of oxidative stress and endothelial dysfunction in ovarian ischemia–reperfusion injury, pharmacological modulation of the NO–sGC–cGMP pathway may represent a promising therapeutic approach. However, the involvement of this signaling pathway in ovarian ischemia–reperfusion injury has not been fully elucidated, and no studies to date have investigated the effects of

riociguat in this setting. Therefore, the aim of the present study was to evaluate the biochemical, hormonal, histopathological, and immunohistochemical effects of riociguat in a rat model of ovarian ischemia–reperfusion injury.

2. Materials and Methods

2.1 Animals and Experimental Design

A total of 47 female Wistar albino rats (220–250 g) were obtained from the Experimental Animal Research Center of Recep Tayyip Erdoğan University (Rize, Türkiye). The animals were housed under standard laboratory conditions (12 h light/dark cycle, 22 ± 2°C) with ad libitum access to food and water. All animals were allowed to acclimatize prior to the experimental procedures.

The rats were randomly assigned into six groups: Control (C) (n = 7), Sham (S) (n = 8), Ischemia (I) (n = 8), Ischemia/Reperfusion (I/R) (n = 8), low-dose riociguat-treated I/R (IRR-3; 3 mg/kg) (n = 8), and high-dose riociguat-treated I/R (IRR-10; 10 mg/kg) (n = 8).

All experimental procedures were approved by the Institutional Animal Care and Use Committee of Recep Tayyip Erdoğan University (Reference No. 202, Decision No. 2024/40, October 23, 2024) and conducted in accordance with established guidelines for the care and use of laboratory animals.

2.2 Experimental Procedure

On the day of the experiment, all animals were weighed and anesthetized via intraperitoneal injection of ketamine hydrochloride (50 mg/kg; Ketalar, Pfizer Pharmaceuticals Inc., İstanbul, Türkiye) and xylazine hydrochloride (10 mg/kg; Rompun, Bayer, USA). Animals remained deeply anesthetized throughout the terminal procedure. No animal regained consciousness prior to euthanasia.

All surgical procedures were performed under sterile conditions. Following a lower midline laparotomy, the ovaries and adnexal structures were exposed. In all groups except the Control and Sham groups, ischemia was induced by applying controlled mechanical compression to the adnexal region.

In the ischemia groups, ovarian ischemia was maintained for 3 hours. In both the ischemia and ischemia/reperfusion (I/R) groups, animals received oral normal saline 90 min after the induction of ischemia. In the I/R groups, reperfusion was established for 3 hours following removal of the vascular clamp after the ischemic period. The Sham group underwent laparotomy without induction of ischemia.

Riociguat (Cat no: AS-19299, Key Organics, UK) was administered via oral gavage at the 90th minute of ischemia. The low-dose group received 3 mg/kg, whereas the high-dose group received 10 mg/kg (19, 20). Administration during the late ischemic phase was selected to allow adequate systemic drug exposure before reperfusion, consistent with experimental ischemia/reperfusion models targeting the pre-reperfusion period for pharmacological intervention. Equivalent volumes of physiological saline were administered via oral gavage to the Sham, Ischemia, and I/R groups.

At the end of the experimental period (total duration: 6 h), anesthesia was confirmed to be adequate by the absence of the pedal withdrawal reflex. Blood samples were collected by cardiac puncture while the animals remained deeply anesthetized. Euthanasia was then performed by intraperitoneal administration of an overdose of ketamine hydrochloride (150 mg/kg) and xylazine hydrochloride (30 mg/kg). Death was confirmed by the absence of heartbeat and spontaneous respiration before bilateral oophorectomy. Every effort was made to minimize animal suffering and the number of animals used.

2.3 Biochemical Analysis

Oxidative stress markers, inflammatory cytokines, and hormonal parameters were evaluated in ovarian tissue and serum samples. Lipid peroxidation levels were determined by measuring thiobarbituric acid reactive substances (TBARS) as an index of malondialdehyde (MDA), using a modified Draper and Hadley method (21). Briefly, following the incubation period, reaction mixtures were cooled in ice for 15 minutes, and the resulting pink chromogen was measured spectrophotometrically at 532 nm. Reduced glutathione (GSH) levels, reflecting antioxidant capacity, were determined using Ellman's reagent method (22). In this assay, tissue supernatants were reacted with DTNB, and absorbance was measured at 412 nm.

Inflammatory parameters, including interleukin-10 (IL-10), interleukin-1 beta (IL-1β), and tumor necrosis factor-alpha (TNF-α), were quantified in ovarian tissue using commercially available enzyme-linked immunosorbent assay (ELISA) kits (Elabscience, USA) in accordance with the manufacturer's instructions.

Hormonal parameters, including luteinizing hormone (LH), follicle-stimulating hormone (FSH), and estradiol (E2) were measured in serum samples obtained from cardiac blood using ELISA kits (Elabscience, USA) according to the manufacturer's protocols.

2.4 Histological Analysis

- Tissue Processing and Sectioning

Ovarian tissues were fixed and dehydrated through a graded ethanol series (70%, 80%, 90%, 96%, and 100%). Following dehydration, tissues were cleared in xylene and embedded in paraffin. Tissue processing was performed using a Shandon Citadel 2000 tissue processor (Thermo Scientific, Germany), and embedding was carried out using a Leica embedding station (EG1150 H and EG1150 C, Germany).

Serial sections of 4–5 µm thickness were obtained using a Leica RM2255 microtome (Germany), floated on a 37°C water bath (Leica HI1210, Germany), and mounted on slides for further analysis.

- **Hematoxylin and Eosin (H&E) Staining**

Sections were deparaffinized, rehydrated, and stained with hematoxylin and eosin using an automated staining system. After dehydration and clearing, the slides were coverslipped using Entellan.

- **Immunohistochemistry**

Ovarian tissue sections mounted on positively charged slides were subjected to deparaffinization, dehydration, and antigen retrieval procedures. The sections were then incubated with primary antibodies against NF-κB p65 (E-AB32233, Elabscience, USA) and NOS3 (eNOS) (E-AB32268, Elabscience, USA) at a dilution of 1:200 at room temperature.

Following secondary antibody incubation, sections were visualized using diaminobenzidine tetrahydrochloride (DAB UltraView, Leica Biosystems, Germany) and counterstained with Harris hematoxylin (Merck KGaA, Germany). Slides were mounted and stored in a dark environment at room temperature.

- **Microscopic Analysis**

Histological and immunostained sections were examined using an Olympus BX51 light microscope equipped with an Olympus DP74 digital camera (Olympus, Japan).

- **TUNEL Assay**

Paraffin sections were deparaffinized following melting at 56°C and subsequently rehydrated. Apoptotic cells were detected using a TUNEL Assay Kit (HRP-DAB, Abcam, ab206386) according to the manufacturer's protocol. Slides were then mounted with Entellan.

- **Histopathological Evaluation**

All H&E-stained ovarian sections were evaluated randomly in five peripheral and one central field per section. Histopathological scoring included degenerative follicles, necrosis, vascular congestion, interstitial edema, polymorphonuclear cell (PMNC) infiltration, stromal hemorrhage, and follicular hemorrhage.

Each parameter was semi-quantitatively scored as follows: 0 (no damage), 1 (mild), 2 (moderate), and 3 (severe) (23, 24).

- **Immunohistochemical Evaluation**

NF-κB p65, NOS3, and TUNEL-stained sections were evaluated using an immunohistochemical positivity scoring system: 0 (< 5%), 1 (6–25%), 2 (26–50%), and 3 (> 50%) (25).

2.5 Statistical Analysis

Statistical analyses were performed using SPSS Statistics version 23 (SPSS Inc., Chicago, IL, USA) and GraphPad Prism version 8.0.2 (GraphPad Software Inc., San Diego, CA, USA). Biochemical data were

analyzed using one-way analysis of variance (ANOVA) with Bonferroni post hoc correction. Normality was assessed using the Shapiro–Wilk test and homogeneity of variances using Levene's test. Histological and immunohistochemical data were analyzed using the Kruskal–Wallis test with post hoc pairwise comparisons. A p-value of < 0.05 was considered statistically significant. Effect sizes for Kruskal–Wallis tests were reported as epsilon squared (ε^2), calculated as $\varepsilon^2 = H / (N - 1)$, and interpreted according to established benchmarks (small ≥ 0.01, medium ≥ 0.08, large ≥ 0.26) (26). A post-hoc power analysis was conducted using G*Power 3.1 (F tests, one-way ANOVA, fixed effects; $f = 0.40$, $\alpha = 0.05$, $N = 47$, $k = 6$), yielding an achieved power of 0.47. This indicates that the study was underpowered relative to the conventional 0.80 threshold, and findings should be interpreted accordingly.

2.6 Use of Artificial Intelligence

During the preparation of this manuscript, the authors used ChatGPT (OpenAI) solely to improve the clarity, readability, language quality, and overall fluency of the text. The AI tool was not used to generate scientific content, analyze or interpret data, or formulate the study's conclusions. All scientific content, analyses, interpretations, and conclusions were critically reviewed, verified, and approved by the authors, who take full responsibility for the final version of the manuscript.

3. Results

3.1 Biochemical Findings

- **Oxidative Stress Parameters**

Oxidative stress markers differed significantly among groups (Table 1). TBARS levels were significantly increased in the ischemia and I/R groups compared with the Control and Sham groups ($p < 0.001$), with the highest levels observed in the I/R group. Riociguat treatment significantly reduced TBARS levels in both treatment groups; however, values did not return to baseline levels (Table 1).

GSH levels showed a significant group difference ($p < 0.001$). While GSH levels remained relatively stable across the Control, Sham, Ischemia, I/R, and IRR-3 groups, a marked and statistically significant increase was observed in the IRR-10 group compared with all other groups (Table 1), indicating a pronounced antioxidant response.

Table 1
Oxidative stress parameters (mean ± SD)

Group	TBARS (nmol/g tissue)	GSH (µmol/g tissue)	
Control	13.70 ± 2.04	1.54 ± 0.36	
Sham	11.65 ± 2.10	1.62 ± 0.30	
Ischemia	63.11 ± 21.05	1.69 ± 0.62	
I/R	77.21 ± 26.61	1.93 ± 0.74	
IRR-3	44.65 ± 11.26	1.72 ± 0.42	
IRR-10	35.30 ± 11.13	3.33 ± 0.91*	
One-Way ANOVA Summary Statistics			
Parameter	**F (df)**	**p**	**Partial η²**
TBARS	F(5,41) = 21.734	< 0.001	0.726
GSH	F(5,40) = 9.616	< 0.001	0.546

Data are presented as mean ± SD.

** GSH IRR-10 group: p < 0.001 vs. all other groups (Bonferroni post hoc correction). TBARS: significant differences were observed between Ischemia and I/R groups vs. Control and Sham groups, and between I/R vs. IRR-3 and IRR-10 groups (p < 0.001); see ANOVA summary statistics below.*

Partial η² = SS_between / SS_total; small ≥ 0.01, medium ≥ 0.06, large ≥ 0.14 (27).

GSH df within = 40 due to one missing value; df reported accordingly.

IRR-3: I/R + Riociguat 3 mg/kg; IRR-10: I/R + Riociguat 10 mg/kg.

- **Hormonal Parameters**

Serum LH, FSH, and estradiol levels showed significant intergroup differences (Table 2). LH levels were significantly elevated in the I/R group compared with all other groups (p < 0.001), and riociguat treatment reduced LH levels toward Control and Sham values (Table 2).

FSH levels showed a significant group difference (p < 0.05). FSH levels were significantly higher in the IRR-10 group compared with the Ischemia, I/R, and IRR-3 groups (p < 0.05). Although FSH levels in the IRR-10 group were numerically higher than those in the Control group, this difference did not reach statistical significance (Table 2).

Estradiol levels were significantly decreased in the Ischemia and I/R groups compared with the Control group (p < 0.05). High-dose riociguat treatment significantly increased estradiol levels in the IRR-10

group compared with the Ischemia and I/R groups ($p < 0.05$), whereas no significant difference was observed between the IRR-10 and Control groups (Table 2).

Table 2
Hormonal profile (mean ± SD)

Group	LH (mIU/mL)	FSH (mIU/mL)	Estradiol (pg/mL)
Control	17.64 ± 2.48	5.19 ± 0.80	1.19 ± 0.13
Sham	15.88 ± 3.59	5.38 ± 1.18	1.11 ± 0.47
Ischemia	20.74 ± 5.16	4.46 ± 0.77	0.91 ± 0.12
I/R	27.40 ± 4.20*	4.55 ± 0.78*	0.73 ± 0.06*
IRR-3	15.14 ± 4.29	4.29 ± 1.03*	0.93 ± 0.18
IRR-10	19.29 ± 4.69	6.42 ± 1.43†	1.69 ± 0.47†
One-Way ANOVA Summary Statistics			
Parameter	**F (df)**	**p**	**Partial η²**
LH	F(5,37) = 7.986	< 0.001	0.519
FSH	F(5,40) = 4.626	0.002	0.366
Estradiol	F(5,37) = 9.768	< 0.001	0.569

Data are presented as mean ± SD.

** p < 0.05 vs. Control group (Bonferroni post hoc correction).*

† p < 0.01 vs. Ischemia and I/R groups (Bonferroni post hoc correction).

FSH: Ischemia vs IRR-10 p = 0.007; I/R vs IRR-10 p = 0.017; IRR-3 vs IRR-10 p = 0.004.

Estradiol: IRR-10 vs Ischemia, I/R, and IRR-3 p = 0.001.

Partial η² = SS_between / SS_total; small ≥ 0.01, medium ≥ 0.06, large ≥ 0.14 (27).

LH and Estradiol df within = 37; FSH df within = 40 (reflecting missing values per variable).

IRR-3: I/R + Riociguat 3 mg/kg; IRR-10: I/R + Riociguat 10 mg/kg.

- **Inflammatory Cytokines**

Inflammatory cytokine analysis revealed a significant increase in IL-10 levels in the IRR-10 group compared with the Ischemia group ($p = 0.001$), suggesting activation of anti-inflammatory pathways

(Table 3). No statistically significant differences were observed among groups in IL-1β or TNF-α levels (Table 3).

Table 3
Inflammatory cytokines (mean ± SD)

Group	IL-10 (ng/g tissue)	IL-1β (ng/g tissue)	TNF-α (ng/g tissue)
Control	1.89 ± 0.45	134 ± 26	1.94 ± 0.56
Sham	1.63 ± 0.31	131 ± 38	1.98 ± 0.83
Ischemia	1.47 ± 0.23	108 ± 10	1.65 ± 0.25
I/R	1.98 ± 0.39	137 ± 34	1.81 ± 0.37
IRR-3	1.76 ± 0.57	133 ± 41	1.77 ± 0.48
IRR-10	2.31 ± 0.49*	135 ± 19	1.94 ± 0.13
One-Way ANOVA Summary Statistics			
Parameter	**F (df)**	**p**	**Partial η²**
IL-10	F(5,41) = 3.833	0.006	0.319
IL-1β	F(5,41) = 1.024	0.416	0.111
TNF-α	F(5,41) = 0.543	0.742	0.062

Data are presented as mean ± SD.

** p = 0.001 vs. Ischemia group (Bonferroni post hoc correction).*

IL-1β and TNF-α: no significant differences among groups (p = 0.416 and p = 0.742, respectively).

Partial η² = SS_between / SS_total; small ≥ 0.01, medium ≥ 0.06, large ≥ 0.14 (27).

IRR-3: I/R + Riociguat 3 mg/kg; IRR-10: I/R + Riociguat 10 mg/kg.

3.2 Histological and Molecular Findings

- **Histopathological Evaluation**

Histopathological scoring revealed significant structural alterations in ovarian tissue following ischemia and reperfusion (Table 4).

Table 4
Histopathological scoring summary (median scores)

Parameter	Control	Sham	Ischemia	I/R	IRR-3	IRR-10
Degenerative follicles	0.33	0.42	1.42*	1.00	0.83	1.09*
Necrosis	0.42	0.67	0.92	0.83	0.83*	0.67
Vascular congestion	0.59	0.92	2.92*	1.17*	1.34*	1.25*
Interstitial edema	0.17	0.25	0.92	1.00*	1.42*	1.33*
PMNC infiltration	0.42	0.42	0.84	0.83	0.83	0.75
Stromal hemorrhage	0	0	1.84*	1.33*	1.34*	1.33*
Follicular hemorrhage	0	0	1.59*	1.17*	0.67*	0.83*
Kruskal–Wallis Summary Statistics						
Parameter	**H**		**p**		**ε²**	
Degenerative follicles	17.90		0.003		0.389	
Necrosis	10.75		0.057		0.234	
Vascular congestion	28.59		< 0.001		0.621	
Interstitial edema	31.45		< 0.001		0.683	
PMNC infiltration	9.19		0.102		0.200	
Stromal hemorrhage	32.81		< 0.001		0.713	
Follicular hemorrhage	31.68		< 0.001		0.688	

Scores represent group medians; semi-quantitative scale: 0 = none, 1 = mild, 2 = moderate, 3 = severe.

** p < 0.05 vs. control/sham group (pairwise post hoc comparison following Kruskal–Wallis test).*

ε² = H / (N − 1); small ≥ 0.01, medium ≥ 0.08, large ≥ 0.26 (26).

PMNC infiltration: H = 9.19, p = 0.102 (not significant overall); ε² = 0.200 indicates medium effect size.

IRR-3: I/R + Riociguat 3 mg/kg; IRR-10: I/R + Riociguat 10 mg/kg; PMNC: polymorphonuclear cell.

Vascular congestion was significantly increased in the Ischemia group compared with Control and Sham groups ($p < 0.001$). Interstitial edema, stromal hemorrhage, and follicular hemorrhage were significantly elevated in I/R and treatment groups compared with Controls ($p < 0.05$) (Table 4, Fig. 1).

Degenerative follicle scores were significantly higher in the Ischemia and IRR-10 groups compared with the Control group ($p < 0.05$). Necrosis scores showed a significant increase only in the IRR-3 group

compared with the Control group (p = 0.0492), while no significant differences were observed in the I/R and IRR-10 groups (Table 4, Fig. 1).

PMNC infiltration showed a numerical increase in the ischemic and I/R groups; however, no statistically significant overall difference was detected among groups (Kruskal–Wallis H = 9.19, p = 0.102, ε² = 0.200) (Table 4, Fig. 1).

- **Immunohistochemical Findings**

Immunohistochemical evaluation demonstrated significant differences in eNOS expression among groups (Table 5, Fig. 2). eNOS expression was significantly higher in the Ischemia group compared with the IRR-10 group (p = 0.0013), indicating modulation of endothelial function following high-dose riociguat treatment (Table 5, Fig. 2).

Table 5
Immunohistochemical and apoptotic findings (median scores)

Group	**eNOS**	**NF-κB**	**TUNEL**
Control	0.75	0.67	0.40
Sham	0.59	0.42	0.40
Ischemia	1.09*	1.30	0.40
I/R	0.50	1.33	0.40
IRR-3	0.50	1.00	0.20
IRR-10	0.17†	0.92	0.20
Kruskal–Wallis Summary Statistics			
Parameter	**H**	**p**	**ε²**
eNOS	16.45	0.006	0.358
NF-κB	—	0.114	—
TUNEL	—	0.822	—

Scores represent group medians; IHC positivity scale: 0 = < 5%, 1 = 6–25%, 2 = 26–50%, 3 = > 50%.

** p < 0.05 vs. Control group (pairwise post hoc comparison following Kruskal–Wallis test).*

† p = 0.0013 vs. Ischemia group (pairwise post hoc comparison following Kruskal–Wallis test).

— : overall Kruskal–Wallis test not significant (p > 0.05); H and ε² not applicable.

ε² = H / (N − 1); small ≥ 0.01, medium ≥ 0.08, large ≥ 0.26 (26).

eNOS: endothelial nitric oxide synthase; NF-κB: nuclear factor kappa B; TUNEL: terminal deoxynucleotidyl transferase dUTP nick end labeling.

No statistically significant differences were observed among groups in NF-κB immunoreactivity or TUNEL positivity (Table 5, Figs. 2 & 3).

4. Discussion

Ovarian torsion represents a complex ischemia–reperfusion (I/R) injury model in which reperfusion paradoxically exacerbates tissue damage. During the ischemic phase, hypoxia, cellular acidosis, and metabolic stress impair ovarian viability, while reperfusion leads to excessive production of reactive oxygen species (ROS) and neutrophil infiltration, further amplifying tissue injury (10, 12, 13). Due to its high metabolic activity, ovarian tissue is particularly susceptible to these alterations. Collectively, this model provides a controlled experimental platform to evaluate early-stage pharmacological modulation of ovarian injury.

In the present study, oxidative stress markers demonstrated a pattern that differed from classical I/R injury models, particularly with respect to GSH responses. Although TBARS levels were significantly elevated in the I/R group, consistent with increased lipid peroxidation (Table 1), riociguat treatment markedly attenuated this increase .

Notably, GSH levels in the high-dose riociguat group were markedly elevated compared with both ischemia and I/R groups, as well as the Control group (Table 1), indicating a supra-normal antioxidant response rather than simple restoration of physiological baseline. This finding may suggest activation of adaptive antioxidant defense mechanisms, potentially involving cGMP-mediated redox regulation pathways. However, the extent of this response also raises the possibility that high-dose riociguat may exert a strong pharmacological modulation of redox homeostasis.

Similar compensatory glutathione responses have been reported in experimental models of ovarian oxidative stress and may reflect an endogenous attempt to restore redox balance under increased oxidative challenge (28–33). Importantly, the observed variability is consistent with moderate-to-large effect sizes in oxidative stress parameters, supporting biological relevance despite limited sample power ($\varepsilon^2 = 0.234$).

These findings indicate that I/R injury is not solely driven by ROS overproduction but also involves dynamic regulation of endogenous antioxidant systems.

Riociguat, through stimulation of the soluble guanylate cyclase (sGC)–cGMP pathway, may improve microcirculation and endothelial function, thereby indirectly reducing oxidative stress and lipid peroxidation (34, 35). Although the observed effects are consistent with activation of the sGC–cGMP pathway, direct confirmation requires measurement of cGMP and downstream signaling molecules.

Histopathological analysis confirmed that vascular alterations constitute a major component of ovarian I/R injury, as evidenced by congestion, edema, hemorrhage, and follicular degeneration (Table 4; Fig. 1), consistent with previous reports (36, 37). Partial improvement following riociguat administration may suggest a protective effect at the microvascular level, potentially related to preservation of endothelial function and vascular homeostasis.

Given the established role of the NO–sGC–cGMP pathway in regulating vascular tone and tissue perfusion, modulation of this pathway may contribute to the observed reduction in oxidative and histopathological injury (36, 37).

A noteworthy histopathological finding was the significantly higher necrosis score observed in the IRR-3 group compared with the Control group ($p = 0.049$), which was not detected in the untreated I/R or IRR-10 groups (Table 4; Fig. 1). This pattern may suggest a non-linear, dose-dependent response to riociguat at the tissue level and should be considered exploratory in nature.

However, this finding should be interpreted cautiously, as the overall Kruskal–Wallis test for necrosis did not reach statistical significance ($H = 10.75$, $p = 0.057$, $\varepsilon^2 = 0.234$). The borderline nature of both global and pairwise comparisons suggests that this observation may reflect statistical fluctuation or heterogeneity within small experimental groups rather than a stable biological effect.

The modest histopathological improvement despite significant biochemical recovery suggests a temporal dissociation between early biochemical adaptation and structural tissue recovery during ischemia–reperfusion injury. Oxidative stress markers such as TBARS and GSH respond rapidly during early reperfusion, whereas inflammatory and structural alterations evolve over a longer time course.

Experimental ischemia–reperfusion studies have demonstrated a biphasic injury pattern in which ROS-mediated damage predominates in the acute phase, while inflammatory and tissue-remodeling processes become more evident during later stages of reperfusion (38). In ovarian I/R injury, vascular congestion, edema, hemorrhage, and follicular degeneration require longer recovery periods (39).

Accordingly, the acute experimental design employed in this study likely captured early biochemical modulation before full histopathological recovery could be observed.

The absence of significant differences in NF-κB and TUNEL staining requires interpretation within the context of reperfusion timing (Table 5; Figs. 2 and 3). This finding may reflect the early phase of reperfusion (3 hours), during which inflammatory and apoptotic pathways may not yet have reached peak activation. Both processes are time-dependent and are typically more pronounced at later reperfusion stages.

In addition, the semi-quantitative immunohistochemical scoring system (0–3 scale) may have limited sensitivity for detecting subtle early changes. NF-κB p65 immunostaining reflects nuclear translocation but does not directly quantify downstream transcriptional activity, which may further contribute to the observed null findings.

The timing of riociguat administration warrants consideration. In the present study, riociguat was administered at the 90th minute of ischemia, prior to reperfusion, to ensure adequate systemic exposure at the onset of reperfusion, consistent with experimental ischemia/reperfusion models targeting this pharmacological window (32).

While this pre-reperfusion strategy is methodologically appropriate for mechanistic interrogation, it differs from the clinical scenario, where intervention would occur after diagnosis and detorsion. Therefore, translational extrapolation should consider this temporal difference in drug exposure.

Furthermore, because riociguat was present during early reperfusion, it may have modulated both oxidative and inflammatory microenvironments during this critical phase, potentially shaping the observed outcomes. Whether pre- or post-reperfusion administration yields equivalent efficacy remains an open experimental question.

From an endocrine perspective, elevated LH levels in the I/R group may reflect altered gonadotropic regulation secondary to impaired steroidogenesis and disrupted ovarian feedback mechanisms (40, 41). Riociguat treatment partially normalized LH levels, suggesting partial restoration of endocrine balance.

Similarly, reductions in FSH and estradiol (E2) in ischemia and I/R groups are consistent with impaired follicular activity and steroid hormone synthesis, whereas partial recovery in the high-dose riociguat group suggests improvement in ovarian steroidogenic function.

Notably, FSH levels in the IRR-10 group exceeded those of the Control group, indicating a supra-baseline gonadotropic response rather than simple normalization. This observation is considered exploratory, and its physiological significance remains to be clarified in future mechanistic studies addressing hypothalamic–pituitary–ovarian axis sensitivity under pharmacological modulation.

Alterations in eNOS expression further indicate endothelial responses to ischemic stress (Table 5; Fig. 2). However, eNOS immunoreactivity does not necessarily reflect functional nitric oxide bioavailability, particularly under conditions of oxidative stress where eNOS uncoupling may occur (14, 35, 42).

The higher eNOS expression observed in the ischemia group may therefore represent a compensatory endothelial response rather than enhanced nitric oxide–mediated vascular function (43–45). In contrast, reduced eNOS expression in riociguat-treated groups despite improved biochemical and hormonal outcomes suggests that vascular protection may be mediated through enhanced downstream signaling efficiency rather than increased enzyme expression.

Beyond its vascular effects, NO–cGMP–PKG signaling has been implicated in ovarian follicular physiology, including regulation of follicular survival and developmental competence through PKG-dependent intracellular pathways (46). In this context, observed eNOS alterations may reflect adaptive endothelial–ovarian signaling shifts during ischemic stress and recovery. However, given that eNOS

immunoreactivity does not directly quantify downstream signaling activity, causal linkage cannot be established from the present dataset.

The observed recovery of estradiol levels may also be linked to preservation of ovarian microvascular function. Ovarian endocrine activity depends critically on vascular homeostasis, as adequate perfusion is required for oxygen delivery, nutrient exchange, and steroid precursor transport to granulosa and theca cells.

Consistent with this concept, studies of controlled ovarian stimulation have demonstrated that increased steroidogenesis is associated with endothelial barrier and vascular adaptations (47). Therefore, preservation of endothelial integrity may have enhanced follicular perfusion and metabolic support, contributing to improved estradiol recovery in riociguat-treated animals.

The absence of significant differences in IL-1β, TNF-α, and NF-κB expression suggests that classical inflammatory pathways may not yet have reached peak activation within the early reperfusion window (3 hours), consistent with the time-dependent nature of cytokine signaling in I/R injury models.

Nevertheless, the increase in IL-10 levels observed in the high-dose riociguat group may indicate early activation of compensatory anti-inflammatory mechanisms, although its biological significance in this acute phase remains to be further elucidated (48, 49).

Taken together, these findings suggest that early-stage ovarian ischemia/reperfusion injury in this model is predominantly characterized by oxidative stress and microvascular dysfunction, with limited detectable activation of classical pro-inflammatory pathways within the examined time frame.

Within this context, riociguat modulates lipid peroxidation, partially preserves histopathological and endocrine parameters, and increases IL-10 levels, collectively indicating a cytoprotective and partially anti-inflammatory effect.

Although these effects are consistent with modulation of the NO–sGC–cGMP signaling axis, the absence of direct measurements of cGMP, nitric oxide bioavailability, and downstream PKG activity precludes definitive mechanistic interpretation. Accordingly, involvement of this pathway should be considered inferential and hypothesis-generating, providing a framework for future time-resolved and mechanistically targeted investigations.

5. Conclusion

Ovarian ischemia–reperfusion injury is a multifactorial process primarily driven by oxidative stress and microvascular dysfunction. In this experimental model, riociguat demonstrated partial protective effects by reducing lipid peroxidation, enhancing antioxidant capacity, improving hormonal balance, and providing partial histological protection.

These effects may be associated with activation of the NO–sGC–cGMP signaling pathway and improved endothelial function, although this mechanism was not directly measured in the present study. While inflammatory and apoptotic markers showed limited changes, the findings suggest that vascular and oxidative mechanisms are the dominant pathways in early ovarian I/R injury.

Riociguat may represent a potential therapeutic approach worthy of further experimental investigation in ovarian torsion–related ischemia–reperfusion injury. However, further studies are required to evaluate long-term reproductive outcomes, optimal dosing strategies, and translational applicability in clinical settings.

6. Limitations

Several aspects of the present study define directions for future investigation. First, activation of the NO–sGC–cGMP pathway was inferred indirectly, as cGMP concentrations, nitric oxide levels, and PKG activity were not directly quantified. Future studies incorporating these molecular endpoints would provide a more comprehensive characterization of riociguat-mediated signaling.

Second, the current experimental design focused on the acute phase of ovarian ischemia–reperfusion injury, evaluating early tissue responses within a limited reperfusion window. Longer-term studies assessing ovarian reserve, ovulatory function, and fertility outcomes are warranted to determine the sustained biological and functional impact of riociguat.

Third, the 3-hour reperfusion period primarily captures early injury dynamics; therefore, delayed inflammatory and apoptotic responses may not have been fully represented. Time-course studies including both early and late reperfusion phases would help to delineate the temporal profile of injury and recovery.

Finally, although several histopathological and biochemical parameters did not reach statistical significance, relatively large effect sizes suggest potential biological relevance that may have been constrained by sample size and statistical power. Future studies with larger cohorts and expanded experimental designs may help to validate and strengthen these observations. In addition, exploration of complementary molecular pathways beyond those assessed in the present study may further elucidate the multifactorial mechanisms underlying the protective effects of riociguat.

Furthermore, the estrous cycle phase was not standardized or recorded prior to the experiments, which may have introduced hormonal variability between individuals, particularly for LH, FSH, and estradiol measurements.

Abbreviations

TBARS
Thiobarbituric Acid Reactive Substances

GSH
Reduced Glutathione
LH
Luteinizing Hormone
FSH
Follicle Stimulating Hormone
IL
Interleukin
TNF-α
Tumor Necrosis Factor-alpha
NF-κB
Nuclear Factor kappa B
eNOS
Endothelial Nitric Oxide Synthase
TUNEL
Terminal deoxynucleotidyl transferase dUTP Nick-End Labeling
NO
Nitric Oxide
sGC
Soluble Guanylate Cyclase
cGMP
Cyclic Guanosine Monophosphate

Declarations

Ethics approval and consent to participate

All experimental procedures involving animals were approved by the Animal Experiments Local Ethics Committee of Recep Tayyip Erdoğan University (Reference No. 202, Decision No. 2024/40, October 23, 2024) and were conducted in accordance with national regulations and institutional guidelines for the care and use of laboratory animals. This study was conducted and reported in accordance with the ARRIVE 2.0 guidelines for reporting animal research.

Consent for publication

Not applicable.

Competing interests

The authors declare that they have no competing interests.

Funding

This work was supported by the Scientific Research Projects Coordination Unit of Recep Tayyip Erdoğan University under Project No. TSA-2025-1996.

Author Contribution

M.A. conceived the study, formulated the research hypothesis, designed the experimental protocol, interpreted the data, and wrote the original draft of the manuscript. E.D. performed the experimental procedures together with M.A. and E.Y.K. and contributed to data acquisition. M.At. performed the biochemical analyses and statistical analysis of the biochemical data together with E.Y.K. Z.T.S performed the histopathological and immunohistochemical evaluations, conducted the statistical analyses of these data, and prepared the histological figures. M.Ö. contributed to the statistical evaluation of the study, critically revised the manuscript for important intellectual content, and supervised the final version of the manuscript. All authors read and approved the final manuscript.

Acknowledgement

The authors thank the staff of the Experimental Animal Research Center of Recep Tayyip Erdoğan University for their technical assistance during the study.

Data Availability

The datasets generated and/or analyzed during the current study are available from the corresponding author upon reasonable request.

References

1. Di Lorenzo G, Mirenda G, Gentile RM, Dal Pozzolo C, Romano F, Ricci G. Use of indocyanine green to evaluate ovarian perfusion after laparoscopic detorsion. A step-by-step demonstration video. Journal of Minimally Invasive Gynecology. 2024;31(4): 269–70.
2. Hibbard LT. Adnexal torsion. American journal of obstetrics and gynecology. 1985;152(4):456–61.
3. Huang C, Hong M-K, Ding D-C. A review of ovary torsion. Tzu-chi medical journal. 2017;29(3):143.
4. Osmanlıoğlu Ş, Saçıntı KG, Aydın M, Şükür YE. Adnexal torsion: a single-center retrospective study of diagnosis and treatment. Anatolian Current Medical Journal. 2023;5(3):282–6.
5. Huchon C, Fauconnier A. Adnexal torsion: a literature review. European Journal of Obstetrics & Gynecology and Reproductive Biology. 2010;150(1):8–12.

6. Sasaki KJ, Miller CE. Adnexal torsion: review of the literature. Journal of minimally invasive gynecology. 2014;21(2):196–202.
7. Dasgupta R, Renaud E, Goldin AB, Baird R, Cameron DB, Arnold MA, et al. Ovarian torsion in pediatric and adolescent patients: a systematic review. Journal of pediatric surgery. 2018;53(7):1387–91.
8. Bayer AI, Wiskind AK. Adnexal torsion: can the adnexa be saved? American journal of obstetrics and gynecology. 1994;171(6):1506–11.
9. Nichols DH, Julian PJ. Torsion of the adnexa. Clinical obstetrics and gynecology. 1985;28(2):375–80.
10. Eltzschig HK, Collard CD. Vascular ischaemia and reperfusion injury. British medical bulletin. 2004;70(1):71–86.
11. Kaleli B, Aktan E, Gezer S, Kirkali G. Reperfusion injury after detorsion of unilateral ovarian torsion in rabbits. European Journal of Obstetrics & Gynecology and Reproductive Biology. 2003;110(1):99–101.
12. Sahin FK, Cosar E, Koken G, Toy H, Basarali K, Buyukbas S. Protective effect of aprotinin on ischemia–reperfusion injury in rat ovary. Journal of Obstetrics and Gynaecology Research. 2008;34(5):794–800.
13. Yavaş ID, Zengin M, Kaklıkaya İ, Uzun Z, Ören A, Elşin MC, et al. Serbest Oksijen Radikal Temizleyici Olarak Aprotinin'in Rolü (Deneysel Çalışma). Türk Göğüs Kalp Damar Cerrahisi Dergisi. 1994;3(2):208–15.
14. Ozcan O, Erdal H, Yonden Z. İskemi-reperfüzyon hasari ve oksidatif stres ilişkisine biyokimyasal bakiş. The Medical Journal of Mustafa Kemal University. 2015;6(23):27–33.
15. Şener G, Yeğen B. İskemi reperfüzyon hasarı. Klinik Gelişim. 2009;22(3):5–13.
16. Mace EH, Kimlinger MJ, Billings IV FT, Lopez MG. Targeting Soluble Guanylyl Cyclase during Ischemia and Reperfusion. Cells. 2023;12(14):1903.
17. Liu R, Kang Y, Chen L. Activation mechanism of human soluble guanylate cyclase by stimulators and activators. Nature communications. 2021;12(1):5492.
18. Conole D, Scott LJ. Riociguat: first global approval. Drugs. 2013;73:1967–75.
19. Al Suleimani YM, Nomeir Y, Al Maskari R, Ali H, Manoj P, Abdelrahman AM. Riociguat Alleviates Cisplatin-Caused Kidney Injury by Suppressing Oxidative Stress and Inflammation. Biology. 2025;14(10):1346.
20. Deniz E, Topcu A, Ozturk A, Ozturk SD, Arpa M, Atak M. The effects of vitamin B12 on the TLR-4/NF-κB signaling pathway in ovarian ischemia-reperfusion injury-related inflammation. Int Immunopharmacol. 2022;107:108676.
21. Draper HH, Hadley M. Malondialdehyde determination as index of lipid Peroxidation. Methods in enzymology. 186: Academic Press, Inc.; 1990. p. 421–31.
22. Ellman G. Tissue sulfhydryl groups. Arch Biochem Biophys. 1959;82:70–7.

23. Kalkan B, Yavuzer B, Aliyev A, Cakir OK, Gozen F, Mendil AS, et al. The molecular mechanism of the protective effect of tianeptine against ovarian ischemia-reperfusion injury. Scientific reports. 2025;15(1):28141.
24. Ulug P, Nayki U, Mammadov R, Bulut S, Tastan TB, Coban TA, et al. Protective effect of Ramipril against oxidant and Proinflammatory cytokine damage induced by Ischemia-Reperfusion in ovarian tissue in rats. Transplantation Proceedings. 2024;56(1):215–22.
25. Suzan ZT, Tumkaya L, Mercantepe T, Atak M, Uydu H. The effect of imatinib administered in the prenatal period on testis development in rats. Human & Experimental Toxicology. 2021;40(4):634–48.
26. Tomczak M, Tomczak E. The need to report effect size estimates revisited. An overview of some recommended measures of effect size. Trends in Sport Sciences, . 2014;1(21):19–25.
27. Cohen J. Statistical power analysis for the behavioral sciences. 2nd ed. United States of America Lawrence Erlbaum Associates, Publishers 1998.
28. Akdemir A, Erbas O, Gode F, Ergenoglu M, Yeniel O, Oltulu F, et al. Protective effect of oxytocin on ovarian ischemia-reperfusion injury in rats. Peptides. 2014;55:126–30.
29. Çolak S, Koc K, Yıldırım S, Geyikoğlu F. Effects of boric acid on ovarian tissue damage caused by experimental ischemia/reperfusion. Biotechnic & Histochemistry. 2022;97(6):415–22.
30. Hizal E, Uyar E, Bingul E, Cicek B, Demir Ö, Mammadov R, et al. The role of antioxidant and anti-inflammatory mechanisms in the protective effects of vigabatrin against ovarian ischemia-reperfusion injury in a rat model. Journal of Ovarian Research. 2025;18(1):214.
31. Öztürk AB, Akaras N, Şimşek H, Kandemir FM. Investigation of the Effects of Silymarin on Ovarian Ischemia Reperfusion via Nrf-2/HO-1/NQO1, Ki-67 and Wnt Signaling Pathways. Journal of Biochemical and Molecular Toxicology. 2025;39(1):e70138.
32. Seker U, Kavak DE, Guzel BC, Baygeldi SB, Yuksel M, Unay Demirel O, et al. Targeting soluble guanylate cyclase with Riociguat has potency to alleviate testicular ischaemia reperfusion injury via regulating various cellular pathways. Andrologia. 2022;54(11):e14616.
33. Sies H. Oxidative stress: a concept in redox biology and medicine. Redox biology. 2015;4:180–3.
34. Ghofrani H-A, Humbert M, Langleben D, Schermuly R, Stasch J-P, Wilkins MR, et al. Riociguat: mode of action and clinical development in pulmonary hypertension. Chest. 2017;151(2):468–80.
35. Stasch J-P, Pacher P, Evgenov OV. Soluble guanylate cyclase as an emerging therapeutic target in cardiopulmonary disease. Circulation. 2011;123(20):2263–73.
36. Gulakar B, Sebin SO, Laloglu E, Tanyeli A, Güler MC, Erbas E, et al. New potential agent in ovarian ischemia reperfusion injury: Alpha pinene. Journal of Biochemical and Molecular Toxicology. 2025;39(6):e70318.
37. Ulas O, Biyik I, Ari NS, Özatik FY, Soysal C, Keskin N, et al. Effects of Vitamin C and Enoxaparin on Ovarian Ischemia–Reperfusion Injury: A Histopathological and Hormonal Evaluation in a Rat Model. Bratislava Medical Journal. 2025;126(12):3395–405.

38. Arab HA, Sasani F, Rafiee MH, Fatemi A, Javaheri A. Histological and biochemical alterations in early-stage lobar ischemia-reperfusion in rat liver. World journal of gastroenterology: WJG. 2009;15(16):1951.
39. Yildirim N, Yigitturk G, Sahingoz Yildirim AG, Akdemir A, İlgen O, Yeniel O, et al. Octreotide protects ovary against ischemia–reperfusion injury in rats: Evaluation of histological and biochemical parameters. Journal of Obstetrics and Gynaecology Research. 2015;41(10):1591–7.
40. Mikhael S, Punjala-Patel A, Gavrilova-Jordan L. Hypothalamic-pituitary-ovarian axis disorders impacting female fertility. Biomedicines. 2019;7(1):5.
41. Valera H, Chen A, Grive KJ. The hypothalamic-pituitary-ovarian axis, ovarian disorders, and brain aging. Endocrinology. 2025;166(10):bqaf137.
42. Förstermann U, Sessa WC. Nitric oxide synthases: regulation and function. European heart journal. 2012;33(7):829–37.
43. Egbert JR, Uliasz TF, Shuhaibar LC, Geerts A, Wunder F, Kleiman RJ, et al. Luteinizing hormone causes phosphorylation and activation of the cGMP phosphodiesterase PDE5 in rat ovarian follicles, contributing, together with PDE1 activity, to the resumption of meiosis. Biology of reproduction. 2016;94(5):110, 1–11.
44. Jaffe LA, Egbert JR. Regulation of mammalian oocyte meiosis by intercellular communication within the ovarian follicle. Annual review of physiology. 2017;79:237–60.
45. Robinson JW, Zhang M, Shuhaibar LC, Norris RP, Geerts A, Wunder F, et al. Luteinizing hormone reduces the activity of the NPR2 guanylyl cyclase in mouse ovarian follicles, contributing to the cyclic GMP decrease that promotes resumption of meiosis in oocytes. Developmental biology. 2012;366(2):308–16.
46. Zhao P, Song Z, Wang Y, Cai H, Du X, Li C, et al. The endothelial nitric oxide synthase/cyclic guanosine monophosphate/protein kinase G pathway activates primordial follicles. Aging (Albany NY). 2020;13(1):1096.
47. Hulde N, Rogenhofer N, Brettner F, Eckert NC, Fetz I, Buchheim J-I, et al. Effects of controlled ovarian stimulation on vascular barrier and endothelial glycocalyx. Journal of Assisted Reproduction and Genetics. 2021;38(9): 2273–82.
48. Moore KW, de Waal Malefyt R, Coffman RL, O'Garra A. Interleukin-10 and the interleukin-10 receptor. Annual review of immunology. 2001;19(1):683–765.
49. Nubbemeyer K, Krabbe J, Böll S, Michely A, Kalverkamp S, Spillner J, et al. Different Effects of Riociguat and Vericiguat on Pulmonary Vessels and Airways. Biomedicines. 2025;13(4):856.

Figures

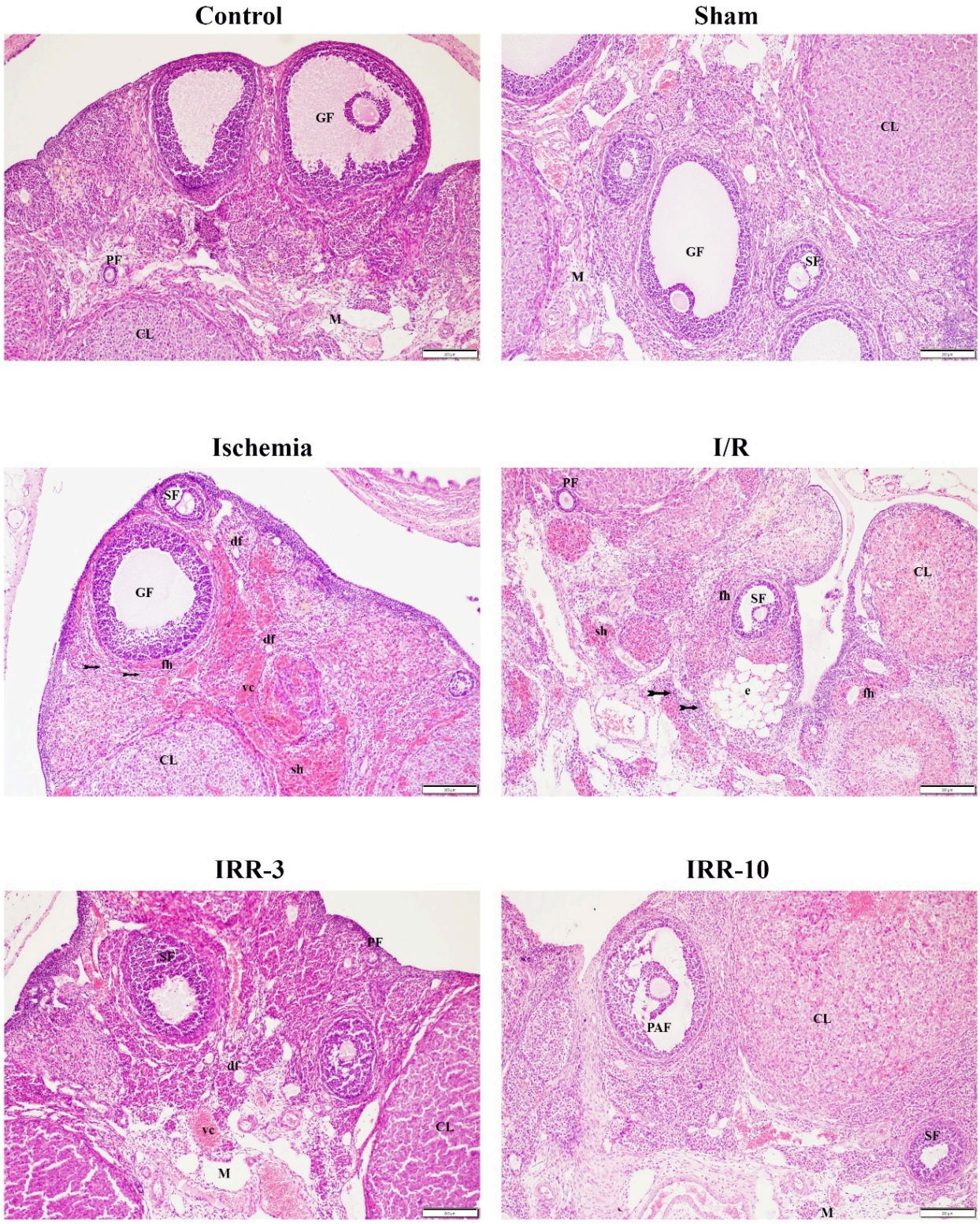


Figure 1

Representative images of ovarian tissues stained with hematoxylin and eosin (×10 magnification). GF: Graafian follicle, SF: secondary follicle, PAF: preantral follicle, PF: primary follicle, M: medulla, fh: follicular hemorrhage, sh: stromal hemorrhage, df: degenerative follicle, e: edema, vc: vascular congestion, pi: PMNC infiltration.

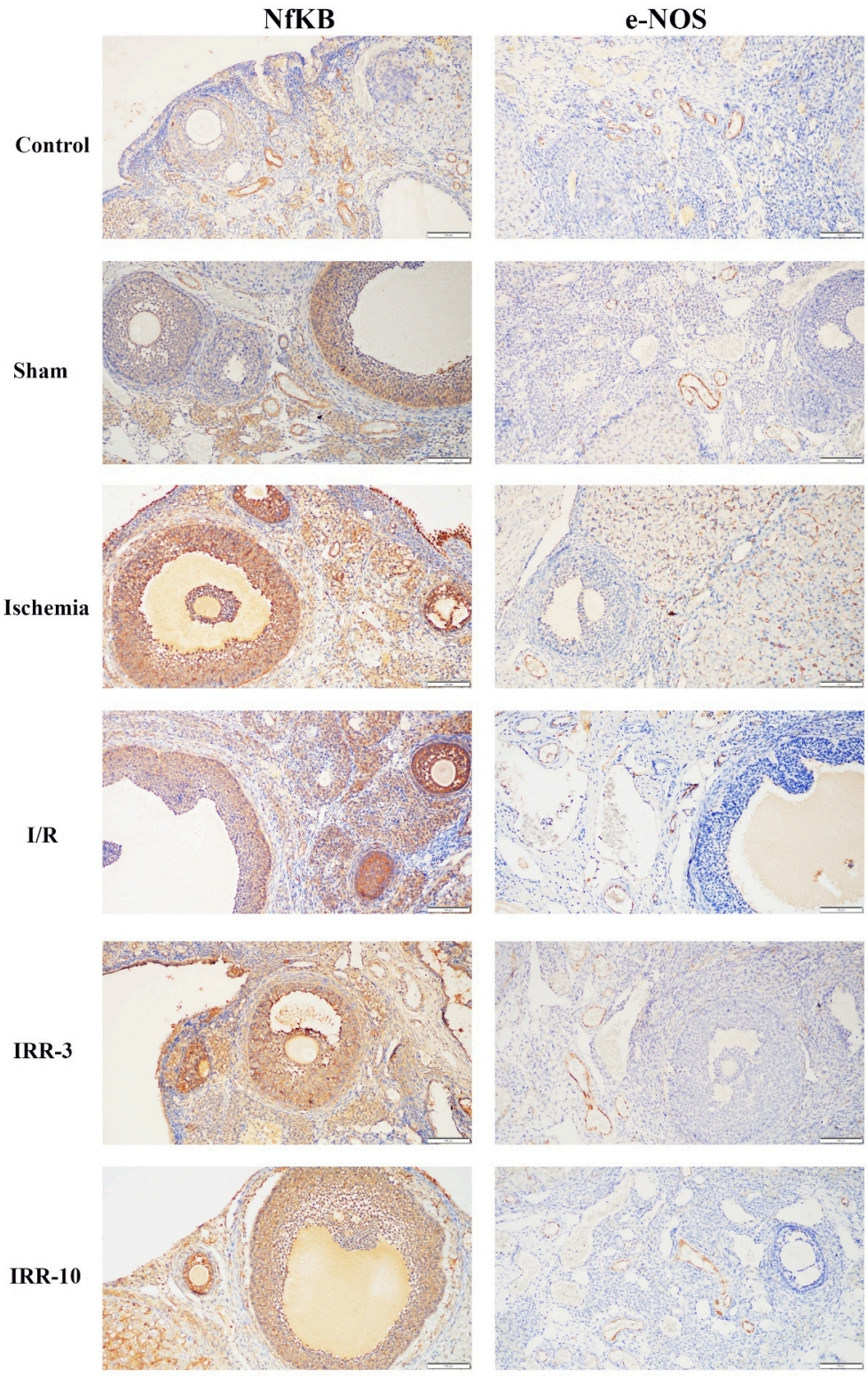


Figure 2

Representative images of ovarian sections immunohistochemically stained with NF-κB and eNOS antibodies (×20 magnification).

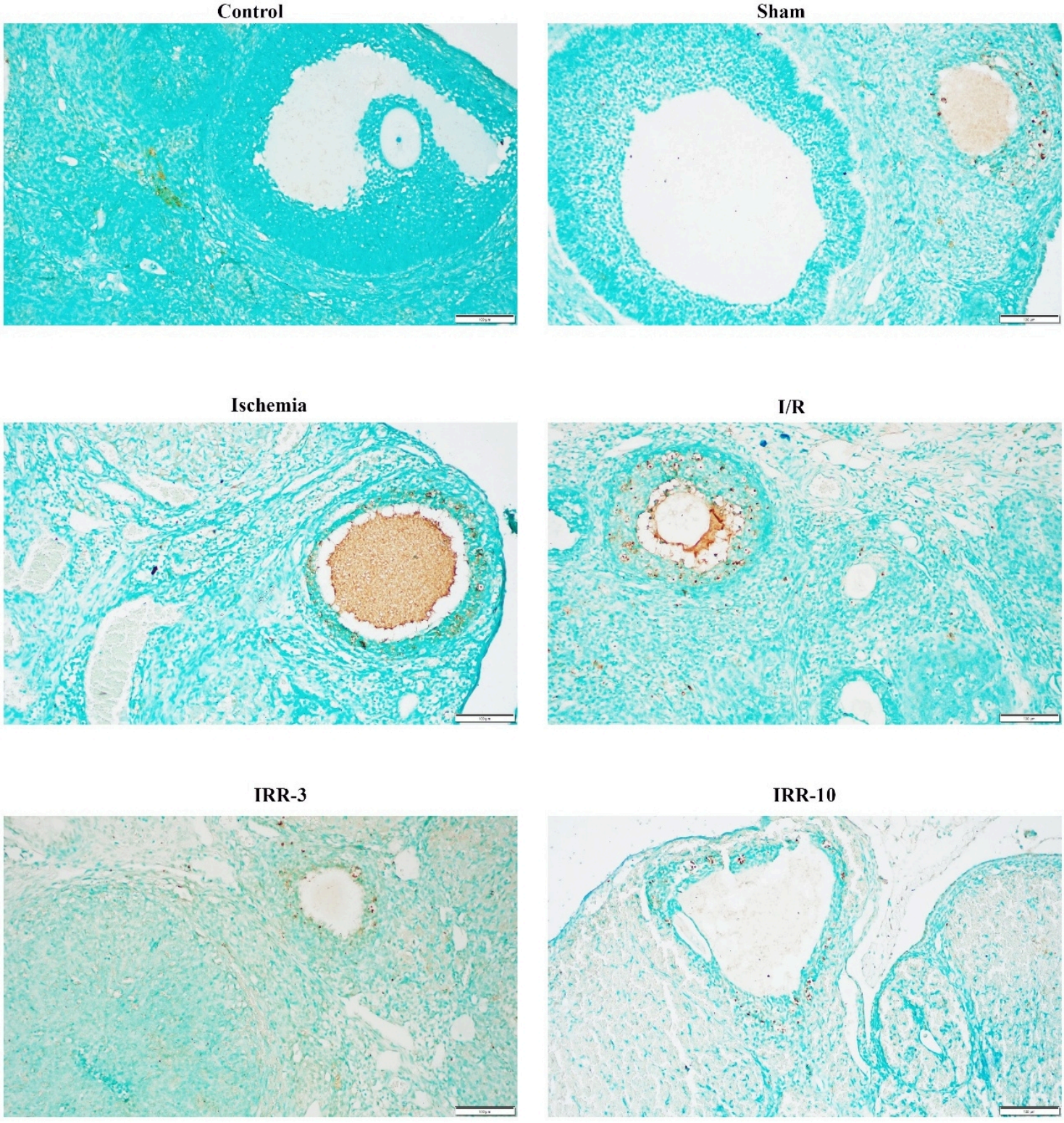


Figure 3

Representative images of ovarian tissues stained using the TUNEL method (×20 magnification).